JACC: CARDIOVASCULAR INTERVENTIONS VOL. 6, NO. 1, 2013

ISSN 1936-8798/$36.00
PUBLISHED BY ELSEVIER INC. http://dx.doi.org/10.1016/j.jcin.2012.09.007

Aortic Root Dimensions Among Patients With Severe Aortic Stenosis Undergoing Transcatheter Aortic Valve Replacement

Lutz Buellesfeld, MD,* Stefan Stortecky, MD,* Bindu Kalesan, PHD,†
Steffen Gloekler, MD,* Ahmed A. Khattab, MD,* Fabian Nietlispach, MD,*
Valentina Delfine, MD,* Christoph Huber, MD,‡ Balthasar Eberle, MD,§
Bernhard Meier, MD,* Peter Wenaweser, MD,* Stephan Windecker, MD*†

Bern, Switzerland

Objectives The aim of this study was to characterize aortic root dimensions of patients with aortic valve stenosis undergoing transcatheter aortic valve replacement (TAVR) and to evaluate sex differences.

Background The advent of TAVR makes a precise delineation of the aortic root anatomy mandatory and requires a profound anatomic understanding.

Methods Patients planned to undergo TAVR underwent screening imaging with use of a 64-slice or dual-source electrocardiogram-gated contrast-enhanced computed tomography. Anatomic dimensions were assessed at the level of the left ventricular outflow tract (LVOT), annulus, sinus of Valsalva, and ascending aorta.

Results The study population comprised 80 men and 97 women (age: 82 $\pm$ 6 years) with symptomatic severe aortic valve stenosis. Multislice computed tomography aortic root assessment revealed larger annular and LVOT dimensions in men than women (area annulus: 483.1 $\pm$ 75.6 mm^2 vs. 386.9 $\pm$ 58.5 mm^2, $p = 0.0002$; area LVOT: 478.2 $\pm$ 131.0 mm^2 vs. 374.0 $\pm$ 94.2 mm^2, $p = 0.0024$), whereas dimensions of the ascending aorta were comparable. Both LVOT and annulus were predominantly oval without sex differences, with a higher mean ellipticity index for the LVOT compared with the annulus (1.49 $\pm$ 0.2 vs. 1.29 $\pm$ 0.1); the ascending aorta was primarily circular (1.07 $\pm$ 0.1). Although similar in mean surface area, an area mismatch of annulus and LVOT of more than 10%, 20%, and 40% was detected in 42, 9, and 2 patients, respectively. The mean distance from annulus to the left coronary ostium was smaller than the mean distance of the right coronary ostium (14.4 $\pm$ 3.6 mm vs. 16.7 $\pm$ 3.6 mm), and distances were lower among women than men.

Conclusions The aortic root has specific anatomic characteristics, which affect device design, selection, and clinical outcome in patients undergoing TAVR. Female sex is associated with smaller annular and LVOT but not aortic dimensions. The degree of ellipticity as well as a significant mismatch between annular and LVOT dimensions in selected patients deserve careful evaluation. (J Am Coll Cardiol Intv 2013;6:72–83) © 2013 by the American College of Cardiology Foundation

From the *Department of Cardiology, Swiss Cardiovascular Center, Bern University Hospital, Bern, Switzerland; †Clinical Trials Unit, Bern, Switzerland; ‡Department of Cardiovascular Surgery, Swiss Cardiovascular Center, Bern University Hospital, Bern, Switzerland; and the §Department of Anesthesiology, Bern University Hospital, Bern, Switzerland. Dr. Buellesfeld is a consultant and proctor for Medtronic. Dr. Khattab has received speaker honoraria and proctor fees from Medtronic CoreValve and Edwards Lifesciences. Dr. Huber has received speaker honoraria and proctor fees from Edwards Lifesciences. Dr. Meier has received research grants from Medtronic and Abbott. Dr. Wenaweser is a proctor and receives honoraria from Medtronic CoreValve and Edwards Lifesciences. Dr. Windecker has received lecture and consultant fees from Edwards Lifesciences and Medtronic CoreValve. All other authors have reported that they have no relationships relevant to the contents of this paper to disclose. Drs. Buellesfeld and Stortecky contributed equally to this work. The Guest Editor for this paper was Peter Block, MD.

Manuscript received June 8, 2012; revised manuscript received August 24, 2012, accepted September 6, 2012.

Due to the rapidly expanding worldwide distribution of transcatheter aortic valve replacement (TAVR), there is an increasing need for a precise anatomic understanding of the aortic root anatomy in which these devices are placed. In contrast to surgical aortic valve replacement, the area of interest is not directly explored by the operator, and therefore TAVR is highly dependent on imaging modalities before and during the procedure. Due to the inability to perform direct annulus sizing and to inspect the proximity to neighboring structures, misjudgment during TAVR might lead to serious complications, including device embolization, coronary occlusion, and device-annulus mismatch, potentially leading to annulus rupture or paravalvular aortic regurgitation.

Among the different imaging modalities, including transthoracic and transesophageal echocardiography, multislice computed tomography (MSCT), and magnet resonance imaging, the capability of 3-dimensional (3D) reconstruction is of paramount importance to fully delineate the aortic root anatomy, because 2-dimensional (2D) techniques are prone to omit important aspects of a 3D structure (1–3). Particularly, MSCT imaging post-processed by a recently released 3D reconstruction tool specifically designed for screening purposes of patients eligible for TAVR has been shown to provide a precise and reproducible assessment of the aortic root structures (4–6).

The aim of the present study was to characterize aortic root anatomy in patients with severe aortic stenosis undergoing TAVR with 3D MSCT reconstruction and to identify sex differences.

Methods

Patient population. This single center study included a consecutive group of patients with severe aortic stenosis evaluated for TAVR who underwent screening by means of MSCT for assessment of the aortic root at our institution. The population comprised a retrospective cohort (TAVR procedure between October 2007 and September 2011) and a prospective cohort (TAVR procedure between August 2011 and March 2012). All patients had an increased surgical risk due to significant comorbidities. The indication to undergo TAVR was based on a consensus by the institutional Heart Team, including experienced clinical and interventional cardiologists, cardiovascular surgeons, and anesthesiologists. All patients provided written informed consent to be included into the TAVR registry.

Study objective. The study objective was to identify and describe anatomic characteristics of the aortic root in defined levels that are relevant for a TAVR procedure. Given the devices available today, specific regions of the aortic root are of interest: the aortic annulus for the purpose of device anchoring and sealing; the left ventricular outflow tract (LVOT) into which the devices extend; the distance of the annular plane to the coronary artery ostia, because coronary obstruction might occur after device placement; the sinus of Valsalva dimensions in which the native leaflets need to fit in, the sino-tubular junction; and the ascending aorta into which self-expanding prostheses, such as the Medtronic CoreValve device, extend for anchoring and coaxial alignment. Therefore, we evaluated the LVOT, annulus, sinus, ascending aorta, and distance of the coronary artery ostia by means of 3D MSCT reconstruction of the aortic root and the ascending aorta.

Imaging technique. The MSCT examinations of the aortic root were performed on either a Siemens Somatom Sensation Cardiac 64 scanner with a slice collimation of 1.5 mm or a Siemens Somatom Definition Flash Dual-Source scanner with a slice collimation of 0.6 mm, tube voltage of 100 or 120 kV, and tube current according to patient size (Siemens Medical Solutions, Inc., Forchheim, Germany). Each patient received an intravenous injection of 80 to 120 ml of contrast medium via the antecubital vein at a flow rate of 5 ml/s. Automated peak enhancement detection in the descending aorta at the level of the diaphragm with a threshold of 100 Hounsfield units was used for timing of the scan. Data acquisition was performed during an inspiratory breath-hold in a craniocaudal direction, whereas the electrocardiogram was recorded simultaneously to allow triggering or retrospective gating. Images were reconstructed at approximately 60% of the RR interval (diastolic phase).

Abbreviations and Acronyms

avD = area-derived virtual diameter

D_{max} = maximum diameter

D_{min} = minimum diameter

EI = ellipticity index

LCA = left coronary artery

LVOT = left ventricular outflow tract

MSCT = multislice computed tomography

pvD = perimeter-derived virtual diameter

RCA = right coronary artery

TAVR = transcatheter aortic valve replacement

2D = 2-dimensional

3D = 3-dimensional

Imaging analysis and definitions. Images were post-processed offline at a dedicated workstation with the automated 3mensio valve software (3mensio Medical Imaging BV, Bilthoven, the Netherlands), a 3D reconstruction tool specifically designed for TAVR screening. Reliability and reproducibility of this software has been reported elsewhere (4–6). After automated reconstruction and segmentation of the aortic root, the annular plane was identified in a perpendicular short-axis view, defined as the plane connecting the nadirs of all 3 aortic cusps (Fig. 1). The LVOT plane was defined as a plane perpendicular to the center line 5 mm below the annular plane; the sinus plane was defined as the plane perpendicular to the centerline that shows the largest cusp dimensions; (the sino-tubular junction) plane, defined as the distal end of the sinus portion; the ascending aorta plane was defined as a plane perpendicular to the center line 30 mm above the annular

JACC: CARDIOVASCULAR INTERVENTIONS, VOL. 6, NO. 1, 2013
JANUARY 2013:72–83

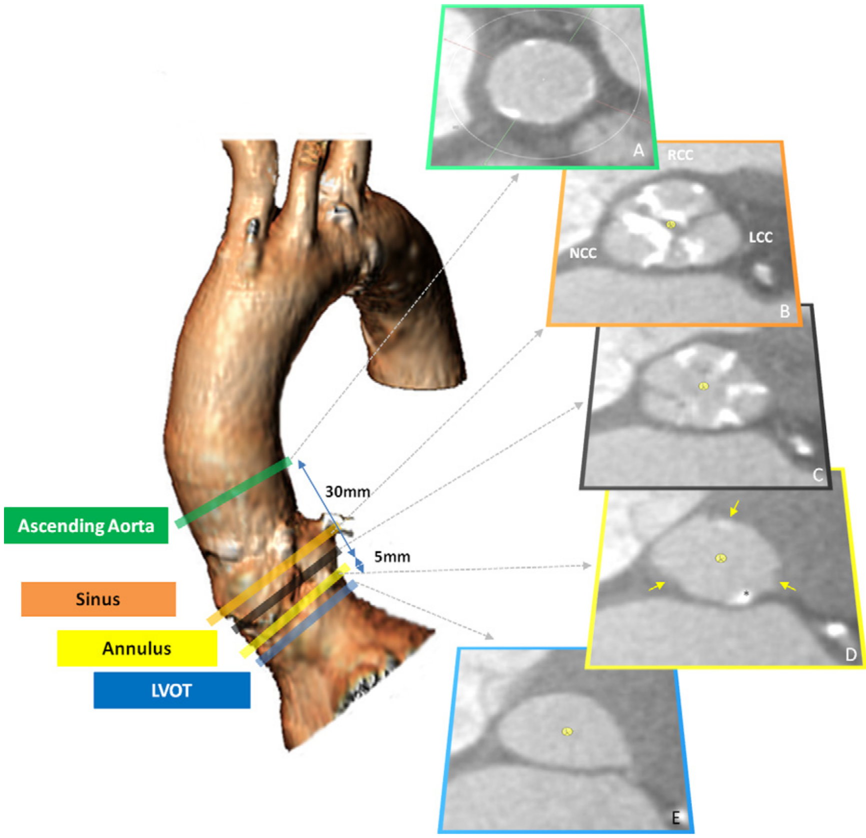

Figure 1. Slicing of the Aortic Root, Demonstrating the Analysis Levels

(A) Ascending aorta, 30 mm above the annular plane. **(B)** Sinus level, showing the coronary cusps. **(C)** Intermediate sinus level (not analyzed). **(D)** Annular plane, defined as plane connecting the nadirs of all 3 cusps. **(E)** Left ventricular outflow tract (LVOT), 5 mm below the annular plane. LCC = left coronary cusp; NCC = noncoronary cusp; RCC = right coronary cusp.

plane. Selection of these specific distances was based on technical device characteristics, because the currently available prostheses heights are between 14 and 55 mm, usually extending more than 5 mm into the LVOT for both the Edwards and Medtronic CoreValve prostheses and up to 50 mm into the ascending aorta for the Medtronic CoreValve prosthesis, which anchors in a region approximately 30 mm above the annular plane.

Multiplanar reformation views stretched along the centerline were used to display the origin of the coronary arteries. Heights of right and left coronary ostia were defined as the distances between the annular plane and the lower border of the ostia in the corresponding view.

Each of the following parameters were obtained in the annular, LVOT, sino-tubular junction, and ascending aorta planes: minimum (D_{min}) and maximum (D_{max}) inner lumen diameters, lumen area and perimeter by manual polygonal border tracing, area-derived virtual diameter (avD) (avD = $\sqrt{[4 \cdot area/\pi]}$), and perimeter-derived virtual diameter (pvD) (pvD = perimeter/π) (Fig. 2). For the sinus of Valsalva, we assessed lumen area and perimeter as well as diameter and height of each cusp. The ellipticity index (EI) was defined as D_{max} divided by D_{min}. Circularity was defined as an EI <1.1, meaning that the difference between D_{max} and D_{min} was <10% of D_{min}.

The analyses were performed independently by 2 experienced observers (L.B. and S.S.) who were blinded to clinical and echocardiographic as well as procedural data.

Statistical analysis. Patient demographic data were prospectively collected and entered in a dedicated database held at the clinical trials unit, Bern, Switzerland. All statistical analyses were performed by a statistician of an academic clinical trials unit (B.K., Clinical Trials Unit, Bern, Bern University Hospital, Switzerland). All continuous measures are presented as mean ± SD, and categorical variables were presented as frequency and percentages. Comparison of baseline and anatomical characteristics between men and women were carried out with Student *t* test for continuous variables and chi-square test or Fisher exact test for categorical variables. Correlation between variables was calcu-

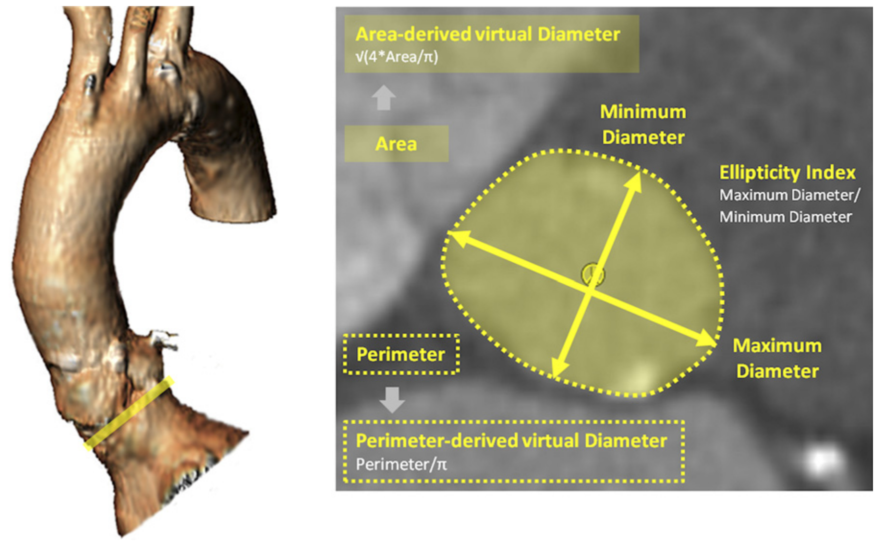

Figure 2. Parameters for Geometric Assessment

As shown for the annular plane, the following parameters were obtained at the various analysis levels: maximum and minimum diameters, area, perimeter, area-derived virtual diameter, perimeter-derived virtual diameter, and ellipticity index.

lated with Pearson's correlation coefficient, and the association between the 2 continuous variables was assessed with linear regression after centering on their mean. The correlation between continuous variables was assessed graphically with scatterplots with confidence ellipses. Additionally, the predicted values from the linear regression were subsequently presented graphically as a fitted line. All statistical tests were 2-sided, and all analysis was performed with Stata (version 11.2, StataCorp, LP, College Station, Texas).

Results

A total of 177 patients were included in this study, and baseline clinical characteristics are summarized in Table 1. Female patients (n = 97, 54.8%) were older than male patients (n = 80, 45.2%), with a mean age of 83.6 ± 4.0 years compared with 81.1 ± 6.5 years ($p = 0.002$). Both patient height and body surface area were larger in men (171.7 ± 7.0 cm vs. 160.7 ± 6.3 cm, $p < 0.0001$; and 1.90 ± 0.2 m^2 vs. 1.72 ± 0.2 m^2, $p < 0.0001$, respectively), whereas body mass indexes were similar (25.4 ± 4.0 kg/m^2 vs. 25.8 ± 4.9 kg/m^2, p = NS). All patients presented with severe aortic valve stenosis (aortic valve area: 0.70 ± 0.2 cm^2 for men, 0.52 ± 0.2 cm^2 for women; $p < 0.0001$). Male patients had a significantly higher risk profile with an increased prevalence of coronary artery disease (77.5% vs. 49.5%; $p < 0.0001$), previous coronary artery bypass graft surgery (31.3% vs. 6.2%; $p < 0.0001$), previous myocardial infarction (22.5% vs. 9.3%; $p = 0.018$) and coronary intervention (38.8% vs. 16.5%; $p = 0.001$), and more severely reduced left ventricular ejection fraction (48.5 ± 14.7% vs. 54.1 ± 15.8%; $p = 0.018$). There were no differences of the functional status (New York Heart Association functional class) as well as the overall risk scores (logistic EuroScore, Society of Thoracic Surgeons Score) between men and women.

Annulus, LVOT, and Sinus of Valsalva

Table 2 displays the overall and sex-specific dimensions of the aortic root. The aortic annulus was significantly larger in men compared with women in terms of area (483.1 ± 75.6 mm^2 vs. 386.9 ± 58.5 mm^2, $p < 0.0001$), perimeter (70.1 ± 6.1 mm vs. 71.0 ± 5.5 mm, $p < 0.0001$), as well as all diameters (e.g., pvD: 25.2 ± 2.0 mm vs. 22.6 ± 1.7 mm, $p < 0.0001$), but EIs were comparable in both groups (1.28 ± 0.1 vs. 1.29 ± 0.1, $p = 0.52$) (Fig. 3). Similarly, the LVOT was significantly larger in men with regard to all parameters (area: 478.2 ± 131.0 mm^2 vs. 374.0 ± 94.2 mm^2, $p < 0.0001$; perimeter: 81.1 ± 11.4 mm vs. 71.8 ± 9.5 mm, $p < 0.0001$; pvD: 25.8 ± 3.6 mm vs. 22.9 ± 3.0 mm, $p < 0.0001$) except the EI, which was similar (1.46 ± 0.2 vs. 1.51 ± 0.2, $p = 0.13$). Overall, the annulus was oval in most patients for both cohorts, with circular shapes (EI ≤1.1) in only 8.8% (7 of 80) of male and 9.3% (9 of 97) of female patients (Fig. 4); in both sex groups as well as the overall population, ellipticity was more pronounced in the LVOT compared with the annulus (1.49 ± 0.2 vs. 1.29 ± 0.1, $p < 0.05$).

In comparisons of annulus and LVOT, there was a sex-independent linear association between annulus and

JACC: CARDIOVASCULAR INTERVENTIONS, VOL. 6, NO. 1, 2013
JANUARY 2013:72–83

Table 1. Baseline Clinical Characteristics

	All (n = 177)	Male (n = 80) (45.2%)	Female (n = 97) (54.8%)	p Value
Age (yrs)	82.5 (5.5)	81.1 (6.5)	83.6 (4.0)	0.002
Height (cm)	165.7 (8.6)	171.7 (7.0)	160.7 (6.3)	<0.0001
Body surface area (m2)	1.80 (0.2)	1.90 (0.2)	1.72 (0.2)	<0.0001
Body mass index (kg/m^2)	25.6 (4.5)	25.4 (4.0)	25.8 (4.9)	0.53
Cardiac risk factors				
Diabetes mellitus	49 (27.7)	20 (25.0)	29 (29.9)	0.47
Hypercholesterolemia	107 (60.5)	53 (66.3)	54 (55.7)	0.15
Hypertension	134 (75.7)	59 (73.8)	75 (77.3)	0.58
Current smoker	22 (12.4)	18 (22.5)	4 (4.1)	0.001
Past medical history				
Myocardial infarction	27 (15.3)	18 (22.5)	9 (9.3)	0.018
Coronary artery bypass graft	31 (17.5)	25 (31.3)	6 (6.2)	<0.0001
Percutaneous coronary intervention	47 (26.6)	31 (38.8)	16 (16.5)	0.001
Stroke	15 (8.5)	8 (10.0)	7 (7.2)	0.51
Peripheral vascular disease	30 (17.0)	17 (21.3)	13 (13.4)	0.17
Chronic obstructive pulmonary disease	28 (16.0)	17 (21.5)	11 (11.5)	0.075
Atrial fibrillation	52 (30.0)	25 (32.5)	27 (27.8)	0.51
Coronary artery disease	110 (62.2)	62 (77.5)	48 (49.5)	<0.0001
Systolic pulmonary artery pressure (mm Hg)	52.7 (17.4)	52.0 (17.4)	53.4 (18.0)	0.6
Aortic valve area (cm^2)	0.60 (0.2)	0.70 (0.2)	0.52 (0.2)	<0.0001
Mean transaortic gradient (mm Hg)	42.8 (17.3)	39.6 (15.2)	45.5 (18.4)	0.029
LVEF (%)	51.6 (15.5)	48.5 (14.7)	54.1 (15.8)	0.018
LVEF ≤50	78 (44.1)	44 (55.0)	34 (35.1)	0.008
LVEF >50	99 (55.9)	36 (45.0)	63 (64.9)	
eGFR (ml/min/1.73 m^2)	54.9 (21.6)	59.3 (22.8)	51.3 (20.0)	0.017
eGFR ≤60	119 (67.2)	50 (62.5)	69 (71.1)	0.22
eGFR >60	58 (32.8)	30 (37.5)	28 (28.9)	
Clinical status				
NYHA			0.57	
Class I	6 (3.4)	3 (3.8)	3 (3.1)	
Class II	57 (32.5)	22 (27.5)	35 (36.1)	
Class III	95 (53.7)	47 (58.7)	48 (49.5)	
Class IV	19 (10.7)	8 (10.0)	11 (11.3)	
Risk assessment				
Logistic EuroScore (%)	23.4 (13.1)	23.5 (13.1)	23.3 (13.5)	0.91
STS score (%)	6.20 (4.0)	5.73 (4.2)	6.60 (3.8)	0.15

Values are n (%).
eGFR = estimated glomerular filtration rate; LVEF = left ventricular ejection fraction; NYHA = New York Heart Association functional class; STS = Society of Thoracic Surgeons.

LVOT size (Fig. 5), and mean dimensions were similar within the subgroups and the overall population. However, a perimeter difference between annulus and LVOT of >10%, 20%, and 40% was detected in 42, 9, and 2 patients, respectively (Fig. 6), indicating a mismatch of annulus and LVOT dimensions in a substantial number of patients.

All sinus of Valsalva dimensions were significantly larger in men compared with women, including area, perimeter, as well as diameters and heights of corresponding cusps (Table 2). In general, in comparisons of the 3 aortic cusps, the noncoronary cusp presented as the largest in terms of diameter, whereas the right coronary cusp was the largest in terms of height. In all patients, the sinus area was larger than the annulus area, with a 15% to 25% area difference in 3 patients, 25% to 50% in 15 patients, and more than 50% in the rest of the population. In comparison of the perimeter-derived virtual annulus diameter with the minimal sinus diameter (defined as the minimum of all 3 cusp diameters), 4 patients had a minimal sinus diameter less than the annulus diameter (Fig. 7).

In general, aortic root dimensions were slightly larger in the prospective group compared with the retrospective group (e.g., pvD annulus: 24.4 ± 2.0 mm vs. 23.5 ± 2.3 mm, p = 0.018), due to the broader inclusion criteria in the

Table 2. Sex-Specific Anatomic Dimensions of the Aortic Root

	All (n = 177)	Male (n = 80) (45.2%)	Female (n = 97) (54.8%)	p Value
Annulus				
Perimeter	74.7 (7.1)	79.1 (6.1)	71.0 (5.5)	<0.0001
Area (mm^2)	430.4 (82.1)	483.1 (75.6)	386.9 (58.5)	<0.0001
Diameter max.	26.2 (2.6)	27.7 (2.4)	25.0 (2.2)	<0.0001
Diameter min.	20.5 (2.3)	21.8 (2.1)	19.4 (1.9)	<0.0001
ΔDiameter	5.73 (2.3)	5.97 (2.3)	5.54 (2.25)	0.22
Ellipticity index	1.29 (0.1)	1.28 (0.1)	1.29 (0.1)	0.52
Virtual diameter (perimeter-derived)	23.8 (2.2)	25.2 (2.0)	22.6 (1.7)	<0.0001
Virtual diameter (area-derived)	23.3 (2.2)	24.7 (1.9)	22.1 (1.7)	<0.0001
Left ventricular outflow tract				
Perimeter	76.0 (11.4)	81.1 (11.4)	71.8 (9.5)	<0.0001
Area (mm^2)	421.1 (123)	478.2 (131)	374.0 (94.2)	<0.0001
Diameter max.	27.9 (4.4)	29.6 (4.5)	26.5 (3.8)	<0.0001
Diameter min.	19.0 (3.1)	20.5 (2.9)	17.8 (2.7)	<0.0001
ΔDiameter	8.90 (3.6)	9.14 (3.9)	8.71 (3.4)	0.43
Ellipticity index	1.49 (0.2)	1.46 (0.2)	1.51 (0.2)	0.13
Virtual diameter (perimeter-derived)	24.2 (3.6)	25.8 (3.6)	22.9 (3.0)	<0.0001
Virtual diameter (area-derived)	22.9 (3.2)	24.5 (3.2)	21.7 (2.7)	<0.0001
Sinus				
Perimeter	103.6 (10.7)	109.3 (9.0)	98.8 (9.6)	<0.0001
Area (mm^2)	772.6 (156.8)	861.5 (138.3)	699.3 (131.6)	<0.0001
Diameter, left coronary cusp	30.8 (3.6)	32.6 (3.1)	29.2 (3.3)	0.0003
Diameter, right coronary cusp	28.7 (3.3)	30.3 (2.7)	27.7 (3.1)	<0.0001
Diameter, noncoronary cusp	31.2 (3.3)	33.0 (3.0)	29.8 (2.9)	<0.0001
Height, average	21.9 (3.0)	23.2 (2.5)	20.9 (2.9)	<0.0001
Height, left coronary cusp	22.0 (3.6)	23.0 (3.1)	21.1 (3.7)	<0.0001
Height, right coronary cusp	22.7 (3.3)	23.8 (3.0)	21.7 (3.2)	<0.0001
Height, noncoronary cusp	21.3 (3.1)	22.7 (2.7)	19.9 (2.9)	<0.0001
Sino-tubular junction				
Perimeter	88.4 (9.6)	92.3 (8.6)	85.2 (9.1)	<0.0001
Area (mm^2)	624.8 (137.5)	679.9 (130.7)	579.3 (126.5)	<0.0001
Diameter max.	29.3 (3.1)	28.3 (2.9)	30.5 (2.8)	<0.0001
Diameter min.	26.9 (3.2)	25.8 (3.0)	28.2 (2.9)	<0.0001
ΔDiameter	2.4 (1.6)	2.4 (1.7)	2.3 (1.6)	0.76
Ellipticity index	1.09 (0.07)	1.10 (0.07)	1.09 (0.06)	0.28
Virtual diameter (perimeter-derived)	28.1 (3.0)	29.4 (2.7)	27.1 (2.9)	<0.0001
Virtual diameter (area-derived)	28.0 (3.0)	29.3 (2.8)	27.0 (2.8)	<0.0001
Coronary ostia				
Height left coronary ostium	14.4 (3.6)	15.1 (3.7)	13.7 (3.4)	0.011
Height right coronary ostium	16.7 (3.6)	17.7 (3.9)	15.9 (3.1)	0.001
Ascending aorta				
Perimeter	92.8 (8.7)	93.9 (8.7)	91.9 (8.7)	0.13
Area (mm^2)	688.0 (133)	704.3 (133)	674.6 (132)	0.14
Diameter max.	30.3 (2.9)	30.5 (3.0)	30.1 (2.9)	0.27
Diameter min.	28.4 (2.7)	28.8 (2.7)	28.1 (2.8)	0.10
Diameter	1.90 (1.4)	1.78 (1.2)	2.00 (1.50)	0.29
Ellipticity index	1.07 (0.1)	1.06 (0.04)	1.07 (0.1)	0.16
Virtual diameter (perimeter-derived)	29.5 (2.8)	29.9 (2.8)	29.2 (2.8)	0.13
Virtual diameter (area-derived)	29.3 (3.5)	29.5 (4.3)	29.2 (2.8)	0.62

Values are millimeters, unless otherwise indicated.

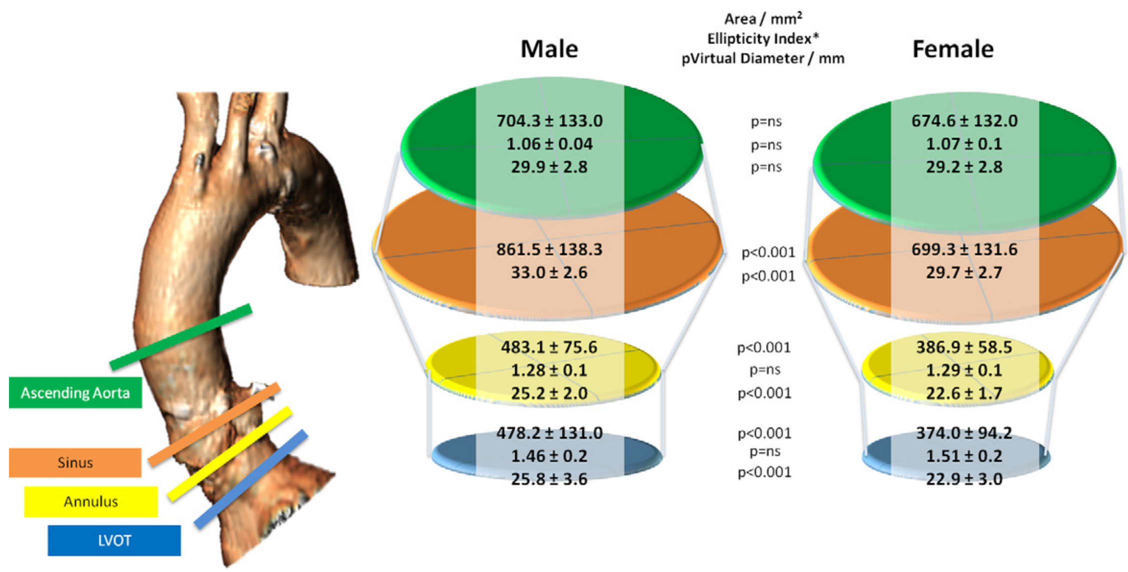

Figure 3. Overview of Sex-Specific Anatomic Aortic Root Dimensions

Comparison of anatomic dimensions of left ventricular outflow tract (LVOT) **(blue)**, aortic valve annulus **(yellow)**, sinus of Valsalva **(orange)**, and ascending aorta **(green)** between men and women. *Not applicable for sinus measurements. pVirtual = perimeter-derived virtual.

prospective phase of the study, given the availability of TAVR prostheses covering a wider range of annulus diameters (Fig. 8), but this did not affect overall results on relative geometric differences at the various levels as well as between both sexes.

Ascending aorta. In contrast to annulus and LVOT, dimensions of the ascending aorta were similar, with a mean area of 704.3 ± 133.0 mm^2 versus 674.6 ± 132.0 mm^2 (p = 0.14), perimeter of 93.9 ± 8.7 mm versus 91.9 ± 8.7 mm (p = 0.13), and pvD of 29.9 ± 2.8 mm versus 29.2 ± 2.8 mm (p = 0.13) for men and women, respectively (Table 2, Fig. 3); in addition, the ascending aorta was predominantly circular in shape compared with both annulus and LVOT (EI 1.07 ± 0.1 vs. 1.29 ± 01 vs. 1.49 ± 0.2, respectively).

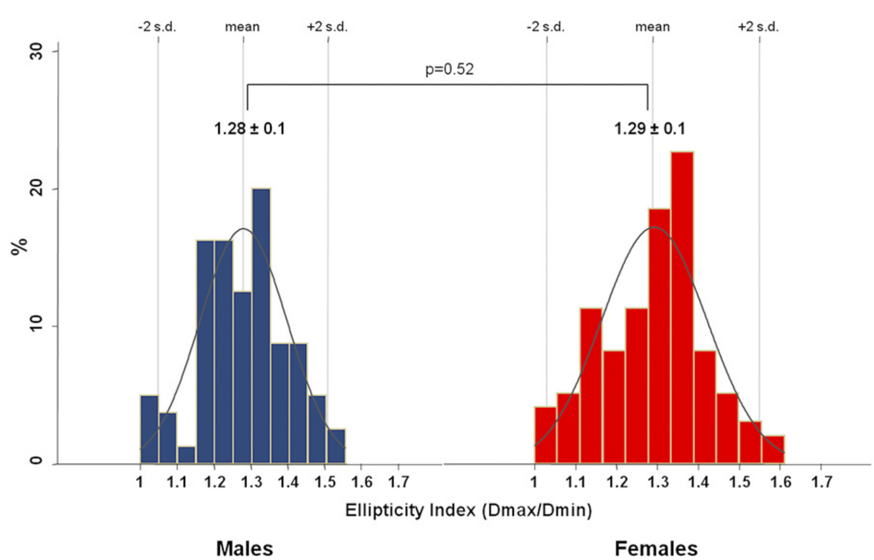

Figure 4. Distribution of Annulus Ellipticity Indexes in Men and Women

Demonstration of similar distribution of the annulus ellipticity index in men **(blue)** and women **(red)**.

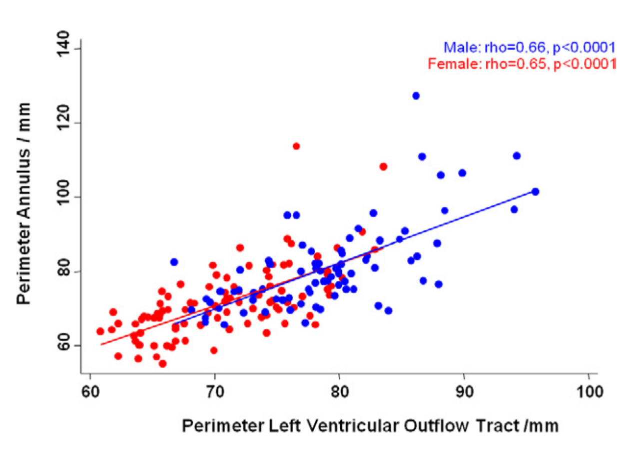

Figure 5. Association of Annulus and LVOT Perimeters

Illustration of geometric relationship between annulus and outflow tract perimeters in men **(blue)** and women **(red)**. LVOT = left ventricular outflow tract.

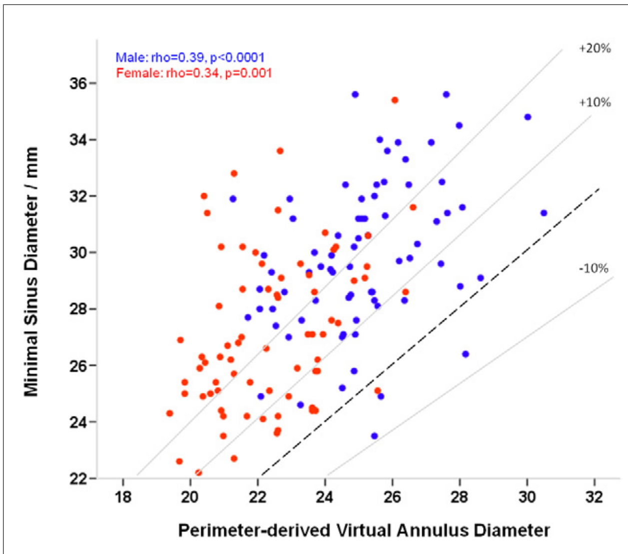

Figure 7. Comparison of Perimeter-Derived Virtual Annulus Diameter and Minimal Sinus Diameter

Lines express the relative difference between perimeter-derived virtual annulus diameter and minimal cusp diameter, indicating larger annulus diameters in 4 patients.

There was no association between annulus size (area or perimeter) and size of the ascending aorta.

Coronary artery height. The average distance of the annular plane to the ostium of the left coronary artery was 15.1 ± 3.7 mm in men and 13.7 ± 3.4 mm in women ($p = 0.011$) and smaller than the average distance to the right coronary ostium (17.7 ± 3.9 mm in men and 15.9 ± 3.1 mm in women, $p = 0.001$). There was no association between the height of the left coronary artery and right coronary artery and no association between the distance of the coronary arteries to the annulus and annular size (Fig. 9).

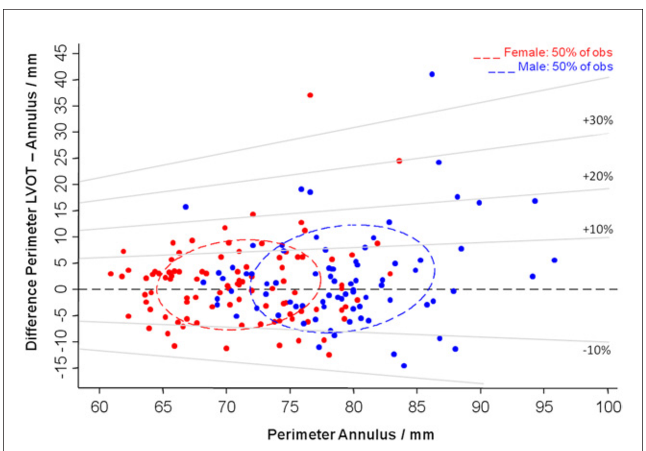

Figure 6. Association of Annulus Perimeters and Corresponding Difference of LVOT and Annulus Perimeters

Lines express the relative difference between left ventricular outflow tract (LVOT) and annulus perimeter, indicating a relative perimeter difference of >10%, 20%, and 40% in 42, 9, and 2 patients, respectively.

Discussion

In the current TAVR era, a precise understanding of aortic root anatomy is critical for device development as well as device selection and implantation to properly address anatomic specifications and avoid complications, such as device embolization, paravalvular regurgitation, annulus rupture, or atrioventricular conduction disturbances. The aortic root is a complex 3D structure whose components have been described in previous reports. Most of these studies evaluated anatomical characteristics on the basis of post-mortem or direct intraoperative inspection, which do not reflect the in vivo geometry of the dynamic aortic root structures, or used 2D imaging modalities, such as echocardiography or conventional MSCT (7–11). However, the latter 2 are affected by the limited ability to describe a 3D structure and are prone to both overestimate and underestimate anatomic structures, because they miss the third dimension.

Our study is the first systematic in vivo evaluation of anatomic dimensions at the various levels of the aortic root in patients with severe aortic stenosis eligible for TAVR with a dedicated 3D MSCT reconstruction tool, which provides standardized "near-anatomic" image post-processing with a high degree of intraobserver and interobserver reproducibility (4–6).

The findings of the present study can be summarized as follows:

Annulus, LVOT, and sinus of Valsalva dimensions are larger in men compared with women, whereas dimensions of the ascending aorta are of similar magnitude.

JACC: CARDIOVASCULAR INTERVENTIONS, VOL. 6, NO. 1, 2013
JANUARY 2013:72–83

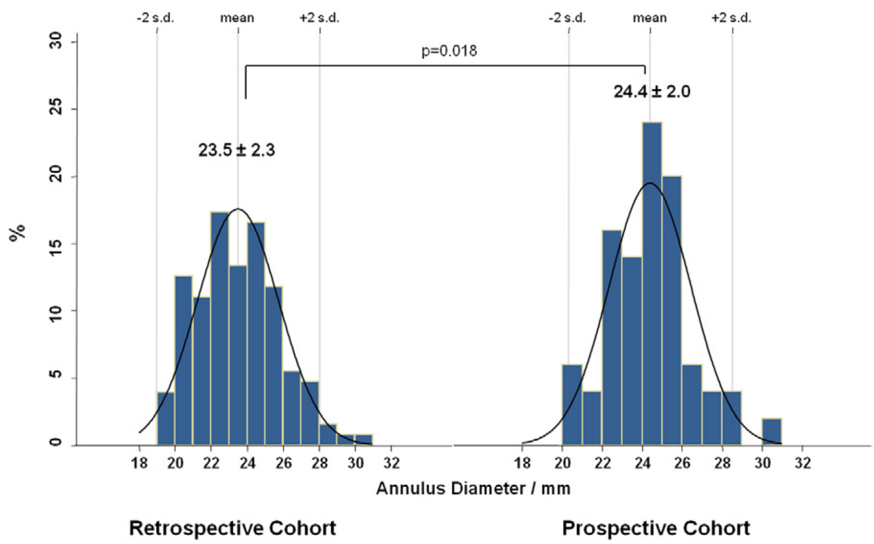

Figure 8. Distribution of Perimeter-Derived Annulus Diameters in Both the Retrospective and Prospective Cohorts

Demonstration of a moderate but significant increase of geometric dimensions, comparing the early retrospective and the late prospective cohorts.

Annulus and LVOT are predominantly oval-shaped without sex differences, whereas the ascending aorta has a circular shape.

There is a geometric mismatch of annulus and LVOT in a relevant number of patients, both with regard to surface area and ellipticity.

There is no association between annulus size and distance to the coronary ostia and no association between the heights of both coronary ostia

We measured the anatomic characteristics at specific levels of the aortic root, namely the annulus, within which the devices are anchored to provide a stable device position and seal without paravalvular regurgitation; the LVOT, defined as a virtual ring 5 mm below the annulus as the area region into which all devices extend; the sinus of Valsalva, which needs to house the native leaflets; and finally the ascending aorta 30 mm above the annulus, where self-expanding prostheses such as the Medtronic CoreValve device extend to provide coaxial alignment.

In comparisons of both sexes, men presented with larger annulus, LVOT, and sinus dimensions, which exceeded those of their female counterparts by 23% to 28% for area-based and 10% to 13% for perimeter-based measures. In contrast, dimensions of the ascending aorta did not reveal sex-specific differences but were similar in both groups. Consequently, there was no association between the annulus area and the area of the ascending aorta for both groups. This is surprising, because one would expect a close correlation between the dimensions of ventricular outflow and the ascending aorta in view of hemodynamic considerations.

Of note, we detected a wide inter individual variability of area sizes at each level with SDs between 58 and 138 mm^2, with an absolute area range of 207 to 930 mm^2 for the LVOT, 286 to 700 mm^2 for the annulus, 490 to 1,220 mm^2 for the sinus, 368 to 1,097 mm^2 for the sino-tubular junction, and 461 to 1,188 mm^2 for the ascending aorta, which complicates geometric predictions and underlines the importance of proper imaging evaluation in each individual patient.

Although the mean surface area of annulus and LVOT were similar and correlated in the overall population as well as within the sex subgroups, the variable distribution among individual patients led to a significant area mismatch between annulus and LVOT of more than 10% in 42 patients, more than 20% in 9 patients, and more than 40% in 2 patients. This finding is important, because a relevant mismatch might have consequences under circumstances where the annulus as a targeted landing zone has been missed, and therefore, the device has to anchor and seal within the LVOT. In cases of significant annulus and LVOT mismatch, a deep implant with a non–straight-tubular device design within a large LVOT will result in significant paravalvular regurgitation due to incomplete paravalvular sealing. Conversely, LVOTs smaller than the corresponding annulus might also have clinical implications, such as LVOT rupture or an increased incidence in conduction disturbances. Therefore, delineation of the anatomy at both the annulus as well as the LVOT level is important to avoid complications or to provide corrective measures in case they ensue. As mentioned in the preceding text, dimensions of the sinus of Valsalva were significantly larger

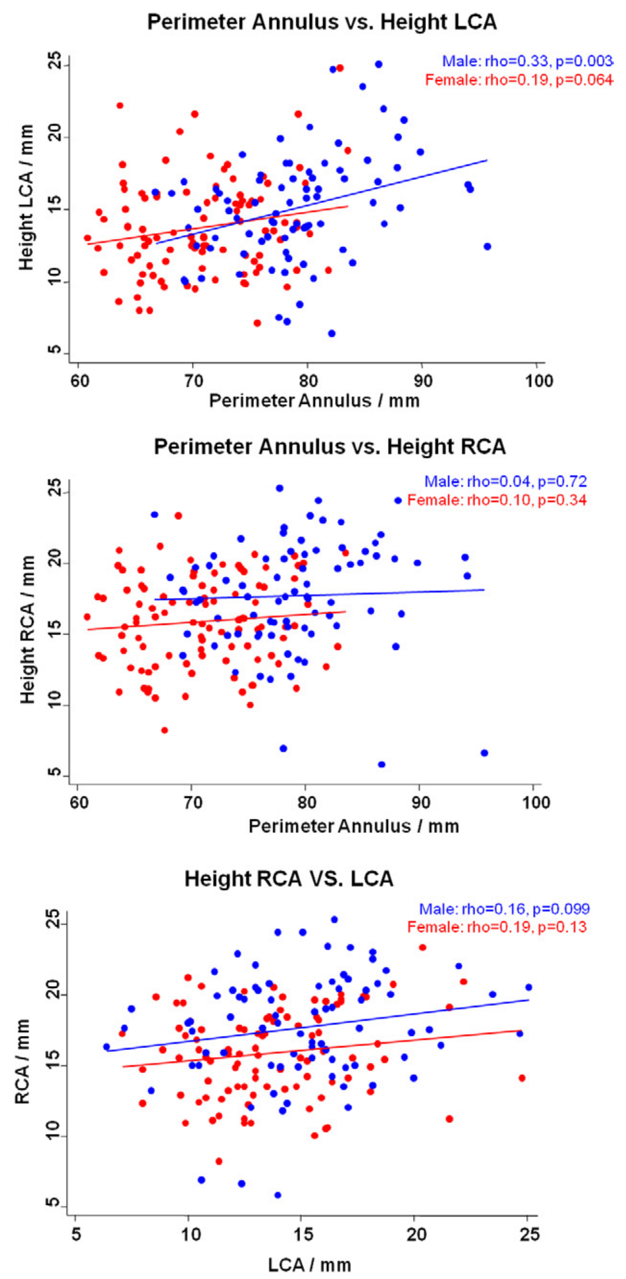

Figure 9. Distance of Coronary Artery Ostium to Annulus

(A) Perimeter annulus and left coronary artery (LCA); **(B)** perimeter annulus and right coronary artery (RCA); and **(C)** LCA and RCA.

in men compared with women, and the sinus area exceeded the annulus area in all cases. However, comparing the virtual annulus diameter with the smallest cusp diameter, we found that the virtual diameter was larger than the minimal cusp diameter in 4 patients (2.3%), and the minimal cusp diameter was only up to 10% larger in 12% of the population, which might be problematic to adequately house the diseased native leaflets, particularly if severe degenerations are present. In the case of the left or right coronary cusp, this geometry, in conjunction with a low coronary take off of, might predispose patients to coronary occlusions.

Annulus and LVOT dimensions showed significant sex-independent differences in shape. In contrast to the ascending aorta, which was fairly circular with a mean EI of 1.07—expressing a 7% difference between maximum and minimum diameters—both annulus and LVOT were primarily oval, which was particularly pronounced at the LVOT level, with an overall EI of 1.49. This resulted in a mean difference between maximum and minimum diameters within the LVOT of 8.9 ± 3.6 mm, compared with an EI of only 1.29 and a mean diameter difference of 5.7 ± 2.3 mm at the annulus level. In other words, the LVOT mean maximum diameter is on average almost 50% larger than the minimum diameter, as opposed to 30% at the annular level. These findings are consistent with previous publications that described the predominance of ovally shaped annuli (12–16), but specific differences of annulus and LVOT have not yet been reported. In addition, these studies were based on 2D techniques only, such as conventional MSCT or echocardiography. Conventional MSCT provides larger dimensions in the coronal than the sagittal view, and these views roughly correspond to the fluoroscopic posterior-anterior projection and the long-axis or 3-chamber views in echocardiography, respectively. These values are routinely reported as maximum and minimum diameters. However, these assessments do not provide a short-axis 3D reconstruction within a clearly defined plane, which is required to identify the true maximum and minimum diameters of a given structure. Therefore, these techniques contain a certain amount of imprecision, and reported values are inconsistent between different techniques (2,3). This in fact might explain why Tops et al. (13), with conventional MSCT, reported oval annulus configurations in only 50% of patients evaluated for TAVR, whereas we observed an ovally shaped annulus in 91% of patients. In addition, annulus and LVOT are dynamic structures with variable ellipticity throughout the cardiac cycle. Just recently, Jilaihawi et al. (15) reported generally larger minimum and mean diameters in systole compared with diastolic measurements, whereas maximum diameters did not significantly change. Consequently, they observed a more circular annular shape in systole, which might be related to the higher peak pressures during this phase of the cardiac cycle. By contrast, several previous reports presented more conflicting and inconsistent findings without a clear association of annular shape and cardiac cycle (17–20). For instance, de Heer et al. (20) noninvasively assessed aortic root dimensions by MSCT reconstruction in both systolic and diastolic phases, which did not reveal significant differences. The individual dimensions actually varied up to 5 mm either way, without sex differences. Therefore, our analysis with diastolic imaging might have traced the morphologies in their most elliptic conformation, but additional studies are needed to exactly address this issue and define the dynamics of morphological changes throughout the cardiac cycle.

The oval conformation, its inter- and intra individual variability, variability of ellipticity at the different levels of the aortic root, as well as the complexity of describing all of these characteristics with the established imaging modalities eventually complicates efforts to standardize correct device selection. Three-dimensional techniques probably have the best capabilities to do so. However, the best parameter on which device selection should be based is yet to be defined. Given the complex anatomy of the aortic root, maximum, minimum, or mean diameters of the annulus alone seem insufficient to act as a sole decision criterion. Calculation of area and perimeter as well as both pvD and avD experiences increasing popularity, and these are concepts that are capable of solving the sizing issue. After implantation of a TAVR prosthesis, the annulus is reshaped toward a more circular geometry (12), and the constant link between the ovally shaped native annulus and the more circular shape after device implantation seems to be the perimeter, which can be translated in the pvD on the basis of the formula (perimeter $= 2 \cdot \pi \cdot r = \pi \cdot$pvD or pvD $=$ perimeter$/\pi$).

Our data demonstrate that the pvD is generally slightly larger than the avD (avD $= \sqrt{[4 \cdot \text{area}/\pi]}$) for all locations and sex groups, and both are in between the maximum and minimum diameters. Safety and efficacy of device selection on the basis of these new parameters is currently being tested in several studies, whose results must be awaited to define the potential of these approaches.

The distance of the annular plane to both coronary ostia is a relevant anatomic parameter, because coronary height below a certain threshold might increase the risk of coronary obstruction (21,22). The mean left coronary artery height was 2.1 to 2.6 mm lower than the right coronary artery, with a mean distance from the annular plane of 14.4 ± 3.6 mm for the left and 16.7 ± 3.6 mm for the right artery. These results corroborate the findings of previous studies based on conventional MSCT assessment and are in line with earlier reports, which identified the right coronary cusp being typically the largest (13,23). In addition, our data demonstrate that the results are sex-dependent, with smaller distances from the annulus for both arteries in women, without correlations between coronary artery height and annulus size or height between left and right coronary artery ostium. Again, because coronary artery height ranges from 6.4 to 25.1 mm for the left and 5.8 to 25.3 mm for the right coronary artery, a precise detection and assessment of these structural characteristics is needed in each individual patient, because predictions are not reliable in view of these wide interindividual differences. Interestingly, post-mortem anatomic analyses found similar results with regard to relative distances, but absolute numbers differed (24). Potential discrepancies in annular plane definitions might explain this observation.

Study limitations. The following limitations of the present study need to be acknowledged: Firstly, this study enrolled patients subsequently undergoing TAVR and does not provide information on aortic root dimensions in an unselected general population. This limitation becomes apparent by the small shift of absolute numbers between the retrospective and the prospective cohorts, which is related to the availability of new prostheses with sizes covering a broader range of annular dimensions. However, these changes did not affect relative sex differences or differences between the different aortic root levels. Secondly, MSCT imaging is known to result in larger annular sizes compared with 2D and 3D echocardiography (2) but seems to provide a good approximation of the true anatomic size, because CT over-sizes compared to echocardiography to a similar extent, in that echocardiography under-sizes the true anatomy, as shown in previous studies (13,25). Thirdly, all measurements were performed in diastole only. Further studies are needed to determine the changes related to the cardiac cycle.

Conclusions

The aortic root is a complex 3D structure with a high degree of intra- and inter individual variability. It has specific anatomic characteristics, which might affect device design, selection, and clinical outcome in patients undergoing TAVR. Female sex is associated with smaller annular and LVOT but not aortic dimensions. Both annulus and LVOT are oval structures with similar surface areas on average. However, the degree of ellipticity as well as significant mismatch between annular and LVOT dimensions in selected patients deserve careful evaluation.

Reprint requests and correspondence: Dr. Lutz Buellesfeld, Department of Cardiology, Swiss Cardiovascular Center Bern, Bern University Hospital, Freiburgstrasse, 3010 Bern, Switzerland. E-mail: lutz.buellesfeld@insel.ch.

REFERENCES

1. Piazza N, de Jaegere P, Schultz C, Becker AE, Serruys PW, Anderson RH. Anatomy of the aortic valvar complex and its implications for transcatheter implantation of the aortic valve. Circ Cardiovasc Interv 2008;1:74–81.
2. Altiok E, Koos R, Schröder J, et al. Comparison of two-dimensional and three-dimensional imaging techniques for measurement of aortic annulus diameters before transcatheter aortic valve implantation. Heart 2011;97:1578–84.
3. Kempfert J, Van Linden A, Lehmkuhl L, et al. Aortic annulus sizing: echocardiographic vs. computed tomography derived measurements in comparison with direct surgical sizing. Eur J Cardiothorac Surg 2012;42:627–33.
4. Schultz CJ, Moelker AD, Tzikas A, et al. Cardiac CT: necessary for precise sizing for transcatheter aortic implantation. EuroIntervention 2010;6 Suppl G:G6–13.

5. de Vaan J, Verstraeten L, de Jaegere P, Schultz C. The 3mensio Valves multimodality workstation. EuroIntervention 2012;7:1464–9.
6. Delgado V, Ng AC, Schuijf JD, et al. Automated assessment of the aortic root dimensions with multidetector row computed tomography. Ann Thorac Surg 2011;91:716–23.
7. Anderson RH, Lal M, Ho SY. Anatomy of the aortic root with particular emphasis on options for its surgical enlargement. J Heart Valve Dis 1996;5 Suppl 3:S249–57.
8. D'Andrea A, Cocchia R, Riegler L, et al. Aortic root dimensions in elite athletes. Am J Cardiol 2010;105:1629–34.
9. Abedin Z, Goldberg J. Origin and length of left main coronary artery: its relation to height, weight, sex, age, pattern of coronary distribution, and presence or absence of coronary artery disease. Cathet Cardiovasc Diagn 1978;4:335–40.
10. Jatene MB, Monteiro R, Guimarães MH, et al. Aortic valve assessment. Anatomical study of 100 healthy human hearts. Arq Bras Cardiol 1999;73:75–86.
11. Kazui T, Izumoto H, Yoshioka K, Kawazoe K. Dynamic morphologic changes in the normal aortic annulus during systole and diastole. J Heart Valve Dis 2006;15:617–21.
12. Ng AC, Delgado V, van der Kley F, et al. Comparison of aortic root dimensions and geometries before and after transcatheter aortic valve implantation by 2- and 3-dimensional transesophageal echocardiography and multislice computed tomography. Circ Cardiovasc Imaging 2010;3:94–102.
13. Tops LF, Wood DA, Delgado V, et al. Noninvasive evaluation of the aortic root with multislice computed tomography implications for transcatheter aortic valve replacement. J Am Coll Cardiol Img 2008; 1:321–30.
14. Doddamani S, Grushko MJ, Makaryus AN, et al. Demonstration of left ventricular outflow tract eccentricity by 64-slice multi-detector CT. Int J Cardiovasc Imaging 2009;25:175–81.
15. Jilaihawi H, Kashif M, Fontana G, et al. Cross-sectional computed tomographic assessment improves accuracy of aortic annular sizing for transcatheter aortic valve replacement and reduces the incidence of paravalvular aortic regurgitation. J Am Coll Cardiol 2012;59:1275–86.
16. Hamdan A, Guetta V, Konen E, et al. Deformation dynamics and mechanical properties of the aortic annulus by 4-dimensional computed tomography: insights into the functional anatomy of the aortic valve complex and implications for transcatheter aortic valve therapy. J Am Coll Cardiol 2012;59:119–27.
17. Messika-Zeitoun D, Serfaty JM, Brochet E, et al. Multimodal assessment of the aortic annulus diameter: implications for transcatheter aortic valve implantation. J Am Coll Cardiol 2010;55:186–94.
18. Schultz C, Rossi A, van Mieghem N, et al. Aortic annulus dimensions and leaflet calcification from contrast MSCT predict the need for balloon post-dilatation after TAVI with the Medtronic CoreValve prosthesis. EuroIntervention 2011;7:564–72.
19. Zhu D, Zhao Q. Dynamic normal aortic root diameters: implications for aortic root reconstruction. Ann Thorac Surg 2011;91:485–9.
20. de Heer LM, Budde RP, Mali WP, de Vos AM, van Herwerden LA, Kluin J. Aortic root dimension changes during systole and diastole: evaluation with ECG-gated multidetector row computed tomography. Int J Cardiovasc Imaging 2011;27:1195–204.
21. Stabile E, Sorropago G, Cioppa A, et al. Acute left main obstructions following TAVI. EuroIntervention 2010;6:100–5.
22. Spiro J, Nadeem A, Doshi SN. Delayed left main stem obstruction following successful TAVI with an Edwards SAPIEN XT valve: successful resuscitation and percutaneous coronary intervention using a non-invasive automated chest compression device (autopulse). J Invasive Cardiol 2012;24:224–8.
23. Berdajs D, Lajos P, Turina M. The anatomy of the aortic root. Cardiovasc Surg 2002;10:320–7.
24. Cavalcanti JS, de Melo NC, de Vasconcelos RS. Morphometric and topographic study of coronary ostia. Arq Bras Cardiol 2003;81:359–62.
25. Babaliaros VC, Liff D, Chen EP, et al. Can balloon aortic valvuloplasty help determine appropriate transcatheter aortic valve size? J Am Coll Cardiol Intv 2008;1:580–6.

Key Words: aortic annulus ■ ascending aorta ■ left ventricular outflow tract ■ transcatheter aortic valve replacement.